

Interference of fractionalized quasiparticles in AIII topological insulators

Carlos G. Velasco and Belén Paredes

*Arnold Sommerfeld Center for Theoretical Physics
Ludwig-Maximilians-Universität München, 80333 München, Germany and
Instituto de Física Teórica CSIC/UAM
C/Nicolás Cabrera, 13-15 Cantoblanco, 28049 Madrid, Spain*

Fractionalization in one-dimensional topological insulators has not been yet directly observed. Moreover, novel symmetry classes of topological insulators like the AIII class lack experimental realization. Our work might open possibilities for both challenges. We propose a one-dimensional model realizing the AIII symmetry class which can be realized in current experiments with ultracold atomic gases. We further report on a remarkable property of topological edge modes: they are localized in momentum space. This opens a path for the direct observation of fractionalization by imaging the momentum distribution of the particles. Furthermore, we exploit the simultaneous sharp definition of the edge modes in position and momentum, to design a quench protocol in which the two halves of an atom move in opposite directions and interfere with each other, preserving their identity as $\frac{1}{2}$ -quasiparticles.

In one dimension the topological or trivial character of an insulator is completely determined by the presence or absence of chiral symmetry [1, 2]. Since chiral symmetry is the composition of time reversal (T) and charge conjugation (C) symmetries, two distinct classes of one-dimensional topological insulators arise: those invariant under T and C, and those breaking both symmetries. The first class, called the BDI symmetry class, is represented by polyacetylene [3–6], which has been the focus of major experimental and theoretical attention. The second class, dubbed the AIII class, has been in contrast rarely explicitly discussed. In a recent interesting connection [7], AIII topological insulators have been proposed to open a physical pathway to Riemann’s conjecture, for one-dimensional models realizing the Riemann zeros seem to belong to the AIII symmetry class. However, AIII topological insulators lack to our knowledge experimental realization.

The topological character of both the BDI and the AIII classes is manifested in the emergence of topologically protected zero energy modes [8], leading to the fascinating phenomena of particle number fractionalization [3–5, 9]. This spectacular property was predicted for polyacetylene by the seminal model of Su, Schrieffer, and Heeger (the SSH model) [5]. At filling factor $\nu = 1/2$, a fermion added to a flat background density splits into two quasiparticles with $1/2$ charge, which are spatially localized at the edges of the one-dimensional system. These quasiparticles are topologically protected robust entities, their fractional quantum numbers being sharp quantum observables as real as the charge of the electron. Though many rather striking properties predicted by the SSH model were confirmed in experiments with polyacetylene, a direct measurement of fractionalization has not been realized yet in one-dimensional topological insulators.

The unique detection possibilities opened up recently with ultracold atoms in optical lattices [10–12] promise to allow for the direct observation of key signatures of topological states such as the Chern number [13, 14], the Berry curvature [15, 16] or the topological edge modes

[17, 18]. For instance, an atomic version of the SSH model has been recently realized [19], and the non trivial Berry phase acquired by a particle when travelling around the Brillouin zone has been directly measured. Furthermore, the control over most parameters promises to enable the quantum simulation of novel classes of topological insulators.

Here, we propose a physical model that realizes a one-dimensional topological insulator in the AIII symmetry class. It can be realized in current experiments with ultracold atoms by combining a superlattice structure [19] with artificial gauge fields [20]. We further report on an unexpected property of topological edge modes in one-dimensional topological insulators: they are surprisingly localized in momentum space as well as they are in position space. This apparently counterintuitive feature indeed resembles what happens for fractions of electrons in fractional quantum Hall liquids [21], which have both well defined position and angular momentum. Exploiting this property we propose a path for the detection of the topological edge modes and fractionalization by imaging the momentum distribution of the particles. This offers an alternative route with respect to previous proposals for the detection of topological edge modes in atomic systems, which are based on the in situ observation of the spacial density [22–25]. Moreover, we show how the simultaneous sharp definition of the position and momentum of edges modes can lead to perfect transport of the fractionalized quasiparticles, which can move preserving their identity without dissipation. We design a quench scenario in which the two halves of an atom move in opposite directions, interfering with each other at the center of the system. They remain localized in position and momentum for long evolution times.

The model. We consider a dimerized lattice model with two sites per unit cell:

$$H = - \sum_n^N \left(J' \hat{a}_n^\dagger \hat{b}_n + J e^{i\delta} \hat{a}_{n+1}^\dagger \hat{b}_n + \text{h.c.} \right), \quad (1)$$

where $\hat{a}_n^\dagger (\hat{b}_n^\dagger)$ are the particle creation operators for a

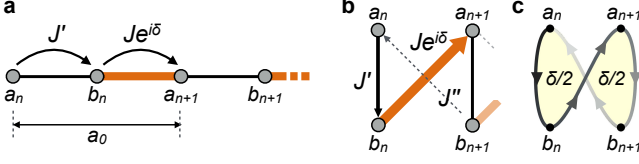


FIG. 1. **The Model.** (a) Schematic illustration of the model for a topological insulator in the AIII class: a one-dimensional dimerized lattice model with two sites a and b per unit cell, and hopping amplitudes J' and $J e^{i\delta}$. The phase δ is a gauge invariant quantity that leads to breaking of time reversal symmetry. This can be seen by deforming the model into a ladder Hamiltonian (b) $H_{\text{Ladder}} = H - J'' \sum_n (\hat{a}_n^\dagger \hat{b}_{n+1} + \text{h.c.})$ in the same symmetry class. Here, the phase δ corresponds to the total phase accumulated along a closed path (c), and thereby to an effective magnetic flux.

particle on the sublattice site $a_n (b_n)$ in the n th lattice cell. For $\delta = 0$ this Hamiltonian corresponds to the SSH model with tunneling amplitudes J and J' [5, 26]. For $\delta \neq 0$ the model introduces a complex phase $e^{i\delta}$ that particles acquire when tunneling from one unit cell to the next [Fig. 1a]. In the presence of this extra phase the model breaks time reversal symmetry, entering the AIII symmetry class. This is better seen by writing the Hamiltonian in momentum space, where it takes the form $H = -J \sum_k \begin{pmatrix} \hat{a}_k^\dagger & \hat{b}_k^\dagger \end{pmatrix} M(k) \begin{pmatrix} \hat{a}_k \\ \hat{b}_k \end{pmatrix}$, with

$$M(k) = [J'/J + \cos(k - \delta)] \sigma_x + \sin(k - \delta) \sigma_y, \quad (2)$$

$\sigma_{x(y,z)}$ being the Pauli matrices. The Hamiltonian exhibits chiral symmetry, since $\sigma_z M(k) \sigma_z = -M(k)$. But for $\delta \neq 0, \pi$ it is not time reversal symmetric (and thereby not charge-conjugation symmetric), for there is no global unitary transformation U such that $U^\dagger M^*(-k) U = M(k)$. It belongs to the AIII class.

The phase δ can not be removed by a gauge transformation. The Hamiltonian for arbitrary δ is connected to the one at $\delta = 0$ through the unitary transformation V :

$$\hat{a}_n^\dagger (\hat{b}_n^\dagger) \xrightarrow{V} e^{-i\delta n} \hat{a}_n^\dagger (\hat{b}_n^\dagger), \quad (3)$$

which is not a gauge transformation. To intuitively understand the physical character of δ it is illuminating to note that the Hamiltonian (1) can be continuously deformed (without changing the symmetry class) into a ladder Hamiltonian with a non-zero magnetic flux per plaquette, which is precisely equal to δ [Fig. 1b,c]. For $\delta = 0$ the magnetic flux vanishes and the system is time reversal symmetric, whereas for $\delta \neq 0$ the magnetic flux leads to a time reversal breaking model in the AIII symmetry class.

The model exhibits a topological phase transition at $J'/J = 1$ [Fig. 2a]. In the trivial phase ($J'/J > 1$) all eigenstates of the Hamiltonian are bulk modes of the form $\hat{c}_{\pm,q}^\dagger \propto \sum_n e^{i\delta n} [\sin(qn - \phi_q) \hat{a}_n^\dagger \pm \sin(qn) \hat{b}_n^\dagger]$, with

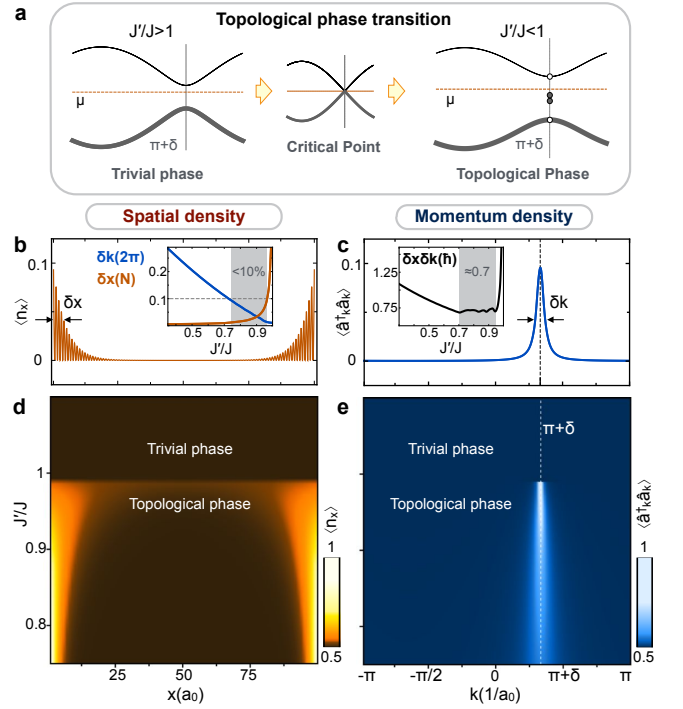


FIG. 2. **Topological edge modes and fractionalization in momentum and position.** (a) Schematic illustration of energy bands in the transition from the trivial to the topological phase. At the critical point the energy gap closes at momentum $\pi + \delta$ and two edge states arise. They are simultaneously localized in position and momentum. (b) Average spatial density $\langle \hat{n}_x \rangle$ and (c) momentum density $\langle \hat{a}_k^\dagger \hat{a}_k \rangle$ of edge modes for $N = 100$, $\delta = -2\pi/3$, and $J'/J = 0.9$. Insets show localization lengths in position and momentum as a function of J'/J . For $0.75 \lesssim J'/J \lesssim 0.95$, both δx (in units of N) and δk (in units of 2π) are smaller than 0.1, with $\delta x \cdot \delta k$ reaching a minimum value of $\sim 0.7\hbar$. (d) Average spacial density and (e) momentum density for the many body state corresponding to a chemical potential $\mu > 0$ such that the upper band is empty. In the topological phase the density profiles show localized peaks (at the edges of the chain, and at momentum $\pi + \delta$) on top of a flat background of density $\nu = 1/2$. This peaks enclose a particle number equal to $1/2$, which is a sharp quantum number (see text).

the momentum q satisfying the quantization condition $q(N + 1) - m\pi = \phi_q$, where $\phi_q = -\text{Arg}(J'/J + e^{-iq})$ and $m = 1, \dots, N$. The modes are distributed in two energy bands of energies $\pm \epsilon(q)$, which are shifted by a momentum δ with respect to the energy bands at $\delta = 0$. At the transition point, the gap closes at $k = \pi + \delta$ and bulk modes with such momentum can not be bound anymore. Two edge modes arise with energies lying in the middle of the gap, which are localized at the ends of the chain [Fig. 2b]:

$$\hat{e}_\pm^\dagger = \frac{1}{\sqrt{2}} \left(\tilde{a}_{n=1}^\dagger \pm \tilde{b}_{n=N}^\dagger \right). \quad (4)$$

Here, $\tilde{a}_{n=1}^\dagger$ is a well localized mode at the left end of the

chain:

$$\hat{a}_{n=1}^\dagger = \sum_n e^{i(\pi+\delta)n} \varphi(n) \hat{a}_n^\dagger, \quad (5)$$

with $\varphi(n) \propto \sinh[\xi(N+1-n)] \approx e^{-\xi n}$ and $\xi \approx -\log(J'/J)$. Similarly, $\hat{b}_{n=N}^\dagger$ is a well localized mode at the right end of the chain.

The "magnetic flux" δ imprints a finite average momentum $k = \pi + \delta$ to the topological edge modes. Surprisingly, the edge modes are well localized around this finite momentum [Fig. 2c]. We have that $\hat{a}_{n=1}^\dagger \equiv \hat{a}_{k=\pi+\delta}^\dagger$, with $\hat{a}_{k=\pi+\delta}^\dagger = \sum_k F(k - \pi - \delta) \hat{a}_k^\dagger$, where $F(k - \pi - \delta)$ is a well localized function around $k = \pi + \delta$ and $F(k) = \frac{1}{\sqrt{N}} \sum_n e^{-ikn} \varphi(n)$. The spatial and momentum localization lengths are $\delta x \simeq \log 2/2\xi$ and $\delta k \simeq 2\xi(1 + \xi^2 N^2 e^{-\xi N})$, respectively. For a wide range of parameters in the topological phase, edge states are simultaneously localized both in position and momentum, satisfying a minimum position-momentum uncertainty [see insets in Fig. 2b,c].

Localization in momentum space opens a path for the detection of topological edge modes by observing the momentum distribution of the corresponding many-body state. For a chemical potential such that the lower band and both edge modes are occupied, the momentum density shows a peak at momentum $\pi + \delta$ on top of a flat background of density $\nu = 1/2$ [Fig. 2e]. The peak encloses a number of particles equal to $1/2$. This fractional particle number is a sharp quantum number, as sharp as the fractionalized particle number at the edges of the chain. To see these properties of the momentum distribution, we consider the corresponding many-body state:

$$|\Phi\rangle = \hat{e}_-^\dagger \hat{e}_+^\dagger \prod_q \hat{c}_{+,q}^\dagger |0\rangle. \quad (6)$$

This state can be written as $|\Phi\rangle = \hat{e}_-^\dagger |\Phi_+\rangle$, where $|\Phi_\pm\rangle = \hat{e}_\pm^\dagger \prod_q \hat{c}_{\pm,q}^\dagger |0\rangle$. The state $|\Phi_+\rangle$, in which all bulk modes in the lower band plus one of the edge states are occupied, has a flat density profile:

$$\nu = \langle \Phi_+ | \hat{a}_k^\dagger \hat{a}_k | \Phi_+ \rangle = \frac{1}{2}. \quad (7)$$

This is easily derived by noticing that $|\Phi_+\rangle$ and $|\Phi_-\rangle$ have the same density profiles:

$$\langle \Phi_+ | \hat{a}_k^\dagger \hat{a}_k | \Phi_+ \rangle = \langle \Phi_- | C^\dagger \hat{a}_k^\dagger \hat{a}_k C | \Phi_- \rangle = \langle \Phi_- | \hat{a}_k^\dagger \hat{a}_k | \Phi_- \rangle,$$

since they are obtained from each other through the unitary transformation C that maps $\hat{a}_n^\dagger \rightarrow \hat{a}_n^\dagger$ and $\hat{b}_n^\dagger \rightarrow -\hat{b}_n^\dagger$. Defining the projectors $P_\pm = \sum_q |q_\pm\rangle \langle q_\pm| + |e_\pm\rangle \langle e_\pm|$, with $|q_\pm\rangle = \hat{c}_{\pm,q}^\dagger |0\rangle$ and $|e_\pm\rangle = \hat{e}_\pm^\dagger |0\rangle$ and taking into account that $P_+ = \mathbb{I} - P_-$, we obtain:

$$\nu = \text{tr}(\hat{a}_k^\dagger \hat{a}_k P_+) = \text{tr}(\hat{a}_k^\dagger \hat{a}_k) - \text{tr}(\hat{a}_k^\dagger \hat{a}_k P_-) = 1 - \nu \quad (8)$$

and thereby $\nu = 1/2$.

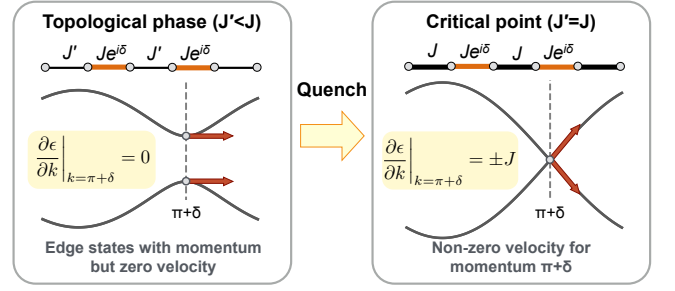


FIG. 3. **Quench to the critical point.** Schematic illustration of Hamiltonians and velocity of edge modes before and after the quench. The edge modes, localized at a momentum $\pi + \delta$ have zero velocity before the quench. They acquire a finite velocity after quenching to the critical point. Since the dispersion relation is linear around the momentum of the edge modes, they can propagate almost without dissipation for long times [Fig. 4].

In the state (6) both edge states are occupied. Therefore the mode $\hat{a}_{n=1}^\dagger = \hat{a}_{k=\pi+\delta}^\dagger$, simultaneously localized in momentum and position is also occupied, and we have:

$$[\hat{a}_{k=\pi+\delta}^\dagger \hat{a}_{k=\pi+\delta} - \nu] |\Phi\rangle = \frac{1}{2} |\Phi\rangle. \quad (9)$$

Thus, a sharp $1/2$ fraction of particles is localized at momentum $k = \pi + \delta$.

Interference of fractional quasiparticles after a quench. The simultaneous sharp definition of momentum and position of the fractional quasiparticles can be exploited to design a scheme in which fractions of atoms move preserving their particle character and interfere with each other without dissipation. We show how such dynamics emerges from quenching of the Hamiltonian to exactly the critical point [Fig. 3]. We consider a situation in which the system is prepared in the state $|\Phi\rangle$ in (6) corresponding to the Hamiltonian H for a certain choice of parameters $J'/J < 1$ and δ . In this state two fractionalized quasiparticles exist at the edges of the chain on top of a flat background of density $\nu = 1/2$. The ratio J'/J is then quenched to the critical point $J'/J = 1$:

$$H(J' < J, \delta) \xrightarrow{\text{Quench}} H(J' = J, \delta), \quad (10)$$

and the system is let evolve in time. The resulting dynamics corresponds to the two quasiparticles moving freely with opposite momentum $\pm(\pi + \delta)$ on top of a flat background density $\nu = 1/2$. This dynamics is a consequence of two facts: *i*) the evolved state $U(t) |\Phi_+\rangle$ keeps its initial flat density distribution at any time, and *ii*) the edge modes propagate almost without dissipation after the quench.

i) Absence of evolution of flat background. The evolved state $U(t) |\Phi_+\rangle$ keeps its flat density at any time and we have:

$$\nu(t) = \langle \Phi_+ | \hat{n}(t) | \Phi_+ \rangle = \frac{1}{2}, \quad (11)$$

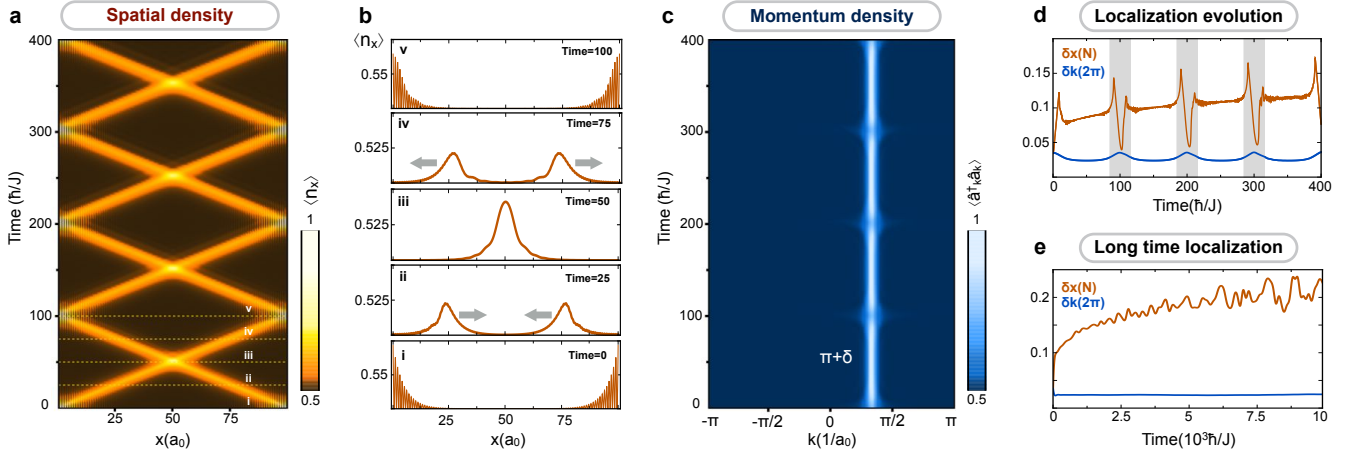


FIG. 4. **Interference of fractionalized quasiparticles.** Time evolution of the many-body state with two fractional quasiparticles after a quench to the critical point. Parameters are $N = 100$ and $\delta = -2\pi/3$. The Hamiltonian is quenched from $J'/J = 0.9$ to $J'/J = 1$. In position space (b) the two quasiparticles keep their definition and move towards the bulk in opposite directions on top of a uniform background of density $\nu = 1/2$. They interfere at the center of the system, travelling back and forth with almost no dissipation. In momentum space (c) quasiparticles keep their sharp momentum $\pi + \delta = \pi/3$. The spatial and momentum localization lengths remain almost constant in time (d, e), with small oscillations occurring when quasiparticles bounce at the edges of the system (d).

where $\hat{n}(t) = U^\dagger(t)\hat{n}U(t)$ and \hat{n} is an arbitrary density operator, either in momentum or position space. To show this we first notice that $U(t)|\Phi_+\rangle$ and $U(t)|\Phi_-\rangle$ have the same density profiles at any time:

$$\begin{aligned} \nu(t) &= \langle \Phi_- | C^\dagger \hat{n}(t) C | \Phi_- \rangle \stackrel{a}{=} \langle \Phi_- | \hat{n}(-t) | \Phi_- \rangle = \\ &\stackrel{b}{=} \langle \Phi_-^{\delta=0} | \hat{n}^{\delta=0}(-t) | \Phi_-^{\delta=0} \rangle \stackrel{c}{=} \langle \Phi_- | \hat{n}(t) | \Phi_- \rangle. \end{aligned} \quad (12)$$

Here, we have used that (a) $C^\dagger H C = -H$ and thereby $C^\dagger U(t) C = U(-t)$. Moreover, we have that (b) expectation values of the density operators are identical to those for the case of $\delta = 0$. Finally, (c) holds because for $\delta = 0$ the Hamiltonian is time reversal symmetric. In addition to (12), using that the evolved projectors $P_+(t)$ and $P_-(t)$ sum to identity at any time, we have:

$$\nu(t) = \text{tr}(\hat{n}P_+(t)) = 1 - \text{tr}(\hat{n}P_-(t)) = 1 - \nu(t), \quad (13)$$

and thus $\nu(t) = 1/2$. In essence, the preservation of the flat background with time is a consequence of the fact that the quench does not change the value of δ . This guarantees that the Hamiltonians before and after the quench are related to the corresponding ones at $\delta = 0$ through the same unitary V defined in (3).

ii) *Free propagation of edge modes.* The edge modes propagate almost freely. This occurs because the dispersion relation of the Hamiltonian at the critical point is linear around the momentum $\pi + \delta$, where the edge modes are localized [Fig. 3]. To study these dynamics it suffices to consider the case $\delta = 0$, since at any time t the evolved edge modes for a given δ are related to the ones at $\delta = 0$ through the unitary V defined in (3):

$$e_\pm(t) = V^\dagger e_\pm^{\delta=0}(t) V. \quad (14)$$

This relation holds because the quench does not change the value of δ and therefore both the initial edge modes and the evolution operator are related to the corresponding ones at $\delta = 0$ through the same V . Since V only introduces a local phase shift it follows that the dynamics of density profiles we derive below for $\delta = 0$ holds for an arbitrary δ .

For $\delta = 0$ the evolution Hamiltonian is given by:

$$H(J' = J, \delta = 0) = -J \sum_{x=1}^{2N} \hat{d}_x^\dagger \hat{d}_{x+1} + \text{h.c.}, \quad (15)$$

where $\hat{d}_{2n-1}^\dagger \equiv \hat{a}_n^\dagger$ and $\hat{d}_{2n}^\dagger \equiv \hat{b}_n^\dagger$, with $n = 1, \dots, N$. The eigenstates of (15) are $\frac{1}{\sqrt{L}} \sum_x \sin qx \hat{d}_x^\dagger$ with eigenvalues $\epsilon(q) = -2J \cos q$, where $q = m\pi/L$, $m = 1, \dots, 2N$ and $2L = N + 1$. We consider the evolution of the mode $\hat{a}_{n=1}^\dagger$ in (5), initially localized at the left edge of the chain. For $\delta = 0$ this mode can be written as:

$$\hat{a}_{n=1}^\dagger = \sum_{x=1}^{2N} \sin \frac{\pi}{2} x \psi(x) \hat{d}_x^\dagger, \quad (16)$$

with $\psi(x) = \varphi(\frac{x+1}{2})$. It is made out of two components: $\sin \frac{\pi}{2} x \psi(x) = \frac{1}{2i} [e^{i\frac{\pi}{2}x} \psi(x) - e^{-i\frac{\pi}{2}x} \psi(x)]$, which have well defined momentum $\pm\pi/2$. It is interesting to analyze how these two components propagate [Fig. 5] forming a localized wave packet that moves with constant velocity towards the bulk, gets reflected at the end of the chain and returns back keeping its localization for long evolution times. First, we show that the $+\pi/2$ component propagates almost freely towards the bulk [Fig. 5]. Defining $G_q = \frac{1}{\sqrt{L}} \sum_x e^{-iqx} \psi(x)$, which is well localized around

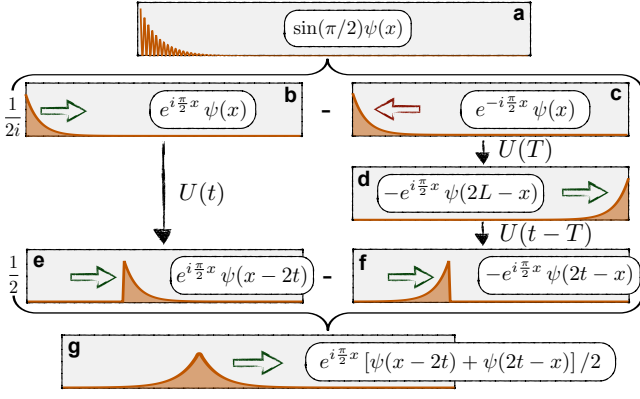


FIG. 5. **Schematic illustration of edge modes dynamics after quench.** A localized edge mode (a) is made out of two components with opposite momenta $+\pi/2$ (b) and $-\pi/2$ (c). The $+$ component propagates towards the bulk (d). The evolution of the $-$ component can be thought as the composition of a reflection (e) at the opposite edge and a time reversed evolution (f). The $-$ component mirrors the density profile of the $+$ component at any time, and the resulting wave packet (f) moves quasi-freely towards the bulk.

momentum zero, we have that:

$$\begin{aligned} U(t)e^{i\frac{\pi}{2}x}\psi(x) &= \frac{1}{2i} \sum_q e^{i2\cos qt} [G_{q-\frac{\pi}{2}} - G_{-q-\frac{\pi}{2}}] \sin qx \\ &\approx \frac{e^{i\pi t}}{2i} \sum_q [e^{-i2qt} G_{q-\frac{\pi}{2}} - e^{i2qt} G_{-q-\frac{\pi}{2}}] \sin qx \\ &= e^{i\frac{\pi}{2}x}\psi(x-2t). \end{aligned} \quad (17)$$

Here, the time t is given in units of \hbar/J and we have used that the dispersion relation is linear around the momenta $\pm\pi/2$, $\epsilon(q) \approx -J\pi \pm 2q$. For a time $t = T$, with $T = L$, the $+\pi/2$ component gets reflected when reaching the right edge [Fig. 5], since we have:

$$U(T)e^{i\frac{\pi}{2}x}\psi(x) = -e^{-i\frac{\pi}{2}x}\psi(2L-x). \quad (18)$$

Using (18) we obtain the evolution of the component with momentum $-\pi/2$:

$$\begin{aligned} U(t)e^{-i\frac{\pi}{2}x}\psi(x) &= U(t-T)U(T)e^{-i\frac{\pi}{2}x}\psi(x) = \\ &= -U(t-T)e^{i\frac{\pi}{2}x}\psi(2L-x) = -e^{i\frac{\pi}{2}x}\psi(2t-x), \end{aligned} \quad (19)$$

which mirrors the density profile of the other component [Fig. 5], composing a wave packet that propagates with constant velocity towards the bulk.

Combining i) and ii) we can conclude that the $\frac{1}{2}$ -quasiparticles preserve their identity over time and we have:

$$[\tilde{a}_{n=1}^\dagger(t)\tilde{a}_{n=1}(t) - \nu]|\Phi(t)\rangle = \frac{1}{2}|\Phi(t)\rangle, \quad (20)$$

where $\tilde{a}_{n=1}^\dagger(t)$ is, as we have shown above, a well localized mode at position $n = t$.

Experimental realization. We develop a scheme [Fig.6] for the realization of the model discussed above. The

scheme combines a superlattice structure [19] together with Raman assisted tunneling [27, 28] to realize a Hamiltonian of the form:

$$H_{\text{exp}} = - \sum_n \left(J' e^{i(2n-1)\delta} \hat{a}_n^\dagger \hat{b}_n + J e^{i2n\delta} \hat{a}_{n+1}^\dagger \hat{b}_n + \text{h.c.} \right).$$

This Hamiltonian is equivalent to our model (1) through the gauge transformation

$$\hat{a}_k^\dagger (\hat{b}_k^\dagger) \longrightarrow \hat{a}_k^\dagger (\hat{b}_{k-2\delta}^\dagger). \quad (21)$$

Interestingly, in the experimental gauge, the momentum distribution of the many body state will show two peaks at positions $\pm(\pi + \delta)$ enclosing a fractionalized $\frac{1}{2}$ -quasiparticle. This fractions could be directly observed by imaging the momentum distribution of the atoms in a time of flight experiment [10].

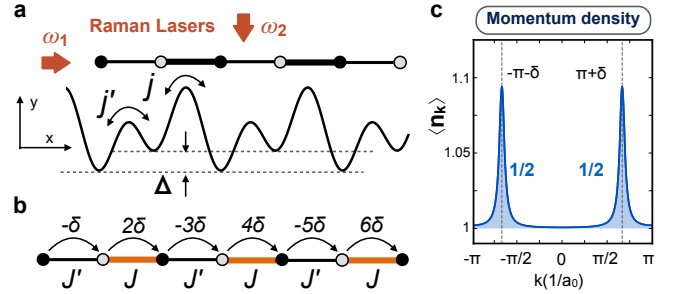


FIG. 6. **Experimental scheme.** (a) A double well potential with energy offset Δ is created from the superposition of two standing waves, forming a one-dimensional lattice with two different tunneling amplitudes j and j' . A pair of Raman lasers is then added along the $-x$ and $-y$ directions with frequency difference $\omega_1 - \omega_2 = \Delta/\hbar$. This leads to a Hamiltonian with position dependent tunneling phases (b), which is gauge-equivalent to our proposed model. (c) The momentum distribution, $\langle \hat{n}_k \rangle = \langle \hat{a}_k^\dagger \hat{a}_k + \hat{b}_k^\dagger \hat{b}_k \rangle$, of the many body state $|\Phi\rangle$ (defined in 6) shows two peaks at positions $\pm(\pi + \delta)$, enclosing a fractionalized $\frac{1}{2}$ -quasiparticle.

In conclusion, we have presented a one-dimensional model realizing the AIII symmetry class which can be readily realized in current experiments. It is a challenge to explore whether variations of this model can serve as physical pathways to Riemann's conjecture [7]. We have reported on a counterintuitive property of topological edge modes in one dimensional topological insulators: they are minimum uncertainty states, simultaneously localized in momentum and position. Our findings open a path for the detection of fractionalization by directly imaging the momentum distribution of the particles. Moreover, the quench protocol we have presented could allow to observe the quantum interference of $\frac{1}{2}$ -fractionalized quasiparticles.

The work of C. G. V. is supported through the grant BES-2013-064443 of the Spanish MINECO.

-
- [1] S. Ryu, A. P. Schnyder, A. Furusaki, and A. W. W. Ludwig, *New J. Phys.* **12**, 065010 (2010).
 - [2] A. Altland and M. R. Zirnbauer, *Phys. Rev. B* **55**, 1142 (1997).
 - [3] R. Jackiw and C. Rebbi, *Phys. Rev. D* **13**, 3398 (1976).
 - [4] J. Goldstone and F. Wilczek, *Phys. Rev. Lett.* **47**, 986 (1981).
 - [5] W. P. Su, J. R. Schrieffer, and A. J. Heeger, *Phys. Rev. Lett.* **42**, 1698 (1979).
 - [6] A. J. Heeger, S. Kivelson, J. R. Schrieffer, and W. P. Su, *Rev. Mod. Phys.* **60**, 781 (1988).
 - [7] G. Sierra, *J. Phys. A: Math. Theor.* **47**, 325204 (2014).
 - [8] J. C. Y. Teo and C. L. Kane, *Phys. Rev. B* **82**, 115120 (2010).
 - [9] S. A. Kivelson, *Synthetic Metals* **125**, 99 (2002).
 - [10] I. Bloch, J. Dalibard, and S. Nascimbène, *Nat. Phys.* **8**, 267 (2012).
 - [11] W. S. Bakr, J. I. Gillen, A. Peng, S. Fölling, and M. Greiner, *Nature* **462**, 74 (2009).
 - [12] J. F. Sherson, C. Weitenberg, M. Endres, M. Cheneau, I. Bloch, and S. Kuhr, *Nature* **467**, 68 (2010).
 - [13] G. Jotzu, M. Messer, R. Desbuquois, M. Lebrat, T. Uehlinger, D. Greif, and T. Esslinger, *Nature* **515**, 237 (2014).
 - [14] M. Aidelsburger, M. Lohse, C. Schweizer, M. Atala, J. T. Barreiro, S. Nascimbène, N. R. Cooper, I. Bloch, and N. Goldman, *Nat. Phys.* **11**, 162 (2015).
 - [15] L. Duca, T. Li, M. Reitter, I. Bloch, M. Schleier-Smith, and U. Schneider, *Science* **347**, 288 (2015).
 - [16] N. Fläschner, B. S. Rem, M. Tarnowski, D. Vogel, D.-S. Lühmann, K. Sengstock, and C. Weitenberg, *Science* **352**, 1091 (2016).
 - [17] M. Mancini, G. Pagano, G. Cappellini, L. Livi, M. Rider, J. Catani, C. Sias, P. Zoller, M. Inguscio, M. Dalmonte, and L. Fallani, *Science* **349**, 1510 (2015).
 - [18] B. K. Stuhl, H.-I. Lu, L. M. Aycock, D. Genkina, and I. B. Spielman, *Science* **349**, 1514 (2015).
 - [19] M. Atala, M. Aidelsburger, J. T. Barreire, D. Abanin, T. Kitagawa, E. Demler, and I. Bloch, *Nat. Phys.* **9**, 795 (2013).
 - [20] J. Dalibard, F. Gerbier, G. Juzeliunas, and P. Öhberg, *Rev. Mod. Phys.* **83**, 1523 (2011).
 - [21] S. M. Girvin, “The quantum hall effect: Novel excitations and broken symmetries,” in *Topological aspects of low dimensional systems* (Springer Berlin Heidelberg, 1999) pp. 53–175.
 - [22] N. Goldman, J. Beugnon, and F. Gerbier, *Phys. Rev. Lett.* **108**, 255303 (2012).
 - [23] N. Goldman, J. Beugnon, and F. Gerbier, *Eur. Phys. J. Special Topics* **217**, 135 (2013).
 - [24] N. Goldman, J. Dalibard, A. Dauphin, F. Gerbier, M. Lewenstein, P. Zoller, and I. B. Spielman, *PNAS* **110**, 6736 (2013).
 - [25] N. Goldman, G. Jotzu, M. Messer, F. Görg, R. Desbuquois, and T. Esslinger, (2016), [arXiv:1606.00015](https://arxiv.org/abs/1606.00015) [cond-mat.quant-gas].
 - [26] P. Delplace, D. Ullmo, and G. Montambaux, *Phys. Rev. B* **84**, 195452 (2011).
 - [27] M. Aidelsburger, M. Atala, S. Nascimbène, S. Trotzky, Y.-A. Chen, and I. Bloch, *Phys. Rev. Lett.* **107**, 255301 (2011).
 - [28] M. Aidelsburger, M. Atala, M. Lohse, J. T. Barreiro, B. Paredes, and I. Bloch, *Phys. Rev. Lett.* **111**, 185301 (2013).